

Successive oxidation stages of adatoms on the Si(111)7×7 surface observed with scanning tunneling microscopy and spectroscopy

J. P. Pelz and R. H. Koch

IBM Research Division, Thomas J. Watson Research Center, P.O. Box 218, Yorktown Heights, New York 10598

(Received 26 February 1990)

Scanning tunneling microscopy and spectroscopy reveal at least a two-stage reaction process which occurs at adatom sites on Si(111)7×7 surfaces exposed to oxygen. Reacted adatoms in the first stage have small ($\sim \frac{1}{2}$ eV) but specific electron-energy shifts, and show roughly a 4:1 preference for the faulted half and a 2:1 preference for the corners of the 7×7 unit cell. Second-stage adatoms appear similar to “missing” adatoms in empty-state topographic images.

For more than two decades, a great deal of experimental¹⁻³ and theoretical^{4,5} work has been done to study the initial oxidation of Si surfaces. Yet considerable uncertainties remain over fundamental questions relating to the location, physical structure, and electronic spectrum of oxidized surface sites, as well as the step-by-step kinetics of the oxidation process. In contrast to most other surface analytical techniques, scanning tunneling microscopy (STM) and the related technique scanning tunneling spectroscopy (STS) offer the capability of probing the structural and electronic properties of surfaces with atomic or near atomic resolution.⁶⁻⁹ To date, however, surprisingly little atomic-resolution STM work on the initial oxidation of Si has been published.^{10,11}

In this paper, we report STM and STS measurements of electronic changes on the Si(111)7×7 surface caused by room-temperature exposure to O₂. Our measurements indicate at least a *two-stage* reaction process of individual Si surface atoms, which appears to nucleate preferentially at certain sites within the 7×7 unit cell. We tentatively assign these two stages to Si surface “adatoms” back bonded to one and two oxygen atoms, respectively. We also report specific spectral features of reacted sites.

Experiments were performed in an ion-pumped UHV chamber with base pressure of roughly 1×10^{-10} Torr, equipped with a quadrupole residual-gas analyzer (RGA). Oxygen dosing was accomplished via a 99.997% pure O₂ source and a precision leak valve. Oxygen pressure (typically 3×10^{-9} Torr during a dose) was determined by monitoring the ion-pump current, previously calibrated against a nude ion gauge. RGA tests indicated that background gas levels (mostly H₂ and CO) measured during typical O₂ doses were too small to account for measured effects. The ion gauge and RGA were turned off during actual experiments to reduce O₂ ionization.

In our custom-built ultrahigh-vacuum STM, the probe tip is scanned via a combination piezoelectric tube and cross assembly, while sample approach as well as lateral positioning was accomplished via a Besocke-type¹² inertial walker. Clean 7×7 surfaces were prepared by quickly heating *n*-type Si(111) wafers to a temperature between 1050 and 1200°C. Either etched W or Pt-Ir tips were used. However, in all cases reported here the tip probably came in contact with the sample before useful data were collected; hence we cannot be certain of the chemical na-

ture of the part of the tip actually involved in the tunneling.

We acquired topographic and spectroscopic data in a manner following Feenstra *et al.*⁷ and Hamers *et al.*⁸ Constant-current topographies with tip bias $V_t \cong -2$ V and tunneling current $I_t \cong 1$ nA were obtained simultaneously with fixed-gap *I-V* curves measured over a voltage range from -2.5 to $+2.5$ V. Usually, 30 *I-V* curves were averaged for each tip location, and a full *I-V* was taken at every point of a 100×100 picture-element (pixel) image covering 20×20 nm². In a typical experiment, we acquired a topograph and a set of *I-V* curves from the clean sample, pulled the tip back ~ 10 – 20 nm, set $V_t \cong 0$ V, dosed the sample with O₂, turned on the tip bias, and reacquired data from the same location. In this way, changes on the surface could be followed on an atom-by-atom basis. As in previous work,¹⁰ our tips were sensitive to oxygen exposure. They would occasionally develop a large electronic band gap and/or lose spatial resolution.

As discussed in a recent review by Hamers,¹³ *I-V* curves can be used to probe the local electronic density of states (DOS) of a sample within a few eV of the Fermi energy E_F . In particular, if one has a *uniform* tip, defined here to be a tip with a nearly constant DOS within a few eV of its Fermi energy, then the quantity $[d \ln I_t / d \ln V_t]_{V_t}$ should be closely related to^{13,14} the sample DOS $\rho_s(E)$ at an energy $E - E_F = -eV_t$. In general, however, there is no *a priori* reason to assume a given tip will, in fact, be uniform. Several recent reports indicate cases where tips probably have significantly nonuniform electronic structure,^{15,16} and our own measurements confirm that different tips can sometimes produce quite different *I-V* curves from equivalent locations on the 7×7 surface. This will be discussed in detail elsewhere.¹⁷

With this in mind, we shall interpret measured *I-V* curves in the following way. First, if a tip does not have a uniform (or known) spectrum, *I-V* curves can still be used simply to indicate that the sample DOS is locally *different* at various parts of a scan. Second, if tips used in particular scans can be shown to be approximately uniform, then *I-V* curves from different parts of these scans can be directly interpreted.

Figures 1(a)–1(d) show a series of empty-state topographic images of a particular region of a sample, successively exposed to a total O₂ dose $D_T \cong 0, 0.1, 0.3, \text{ and } 0.9$

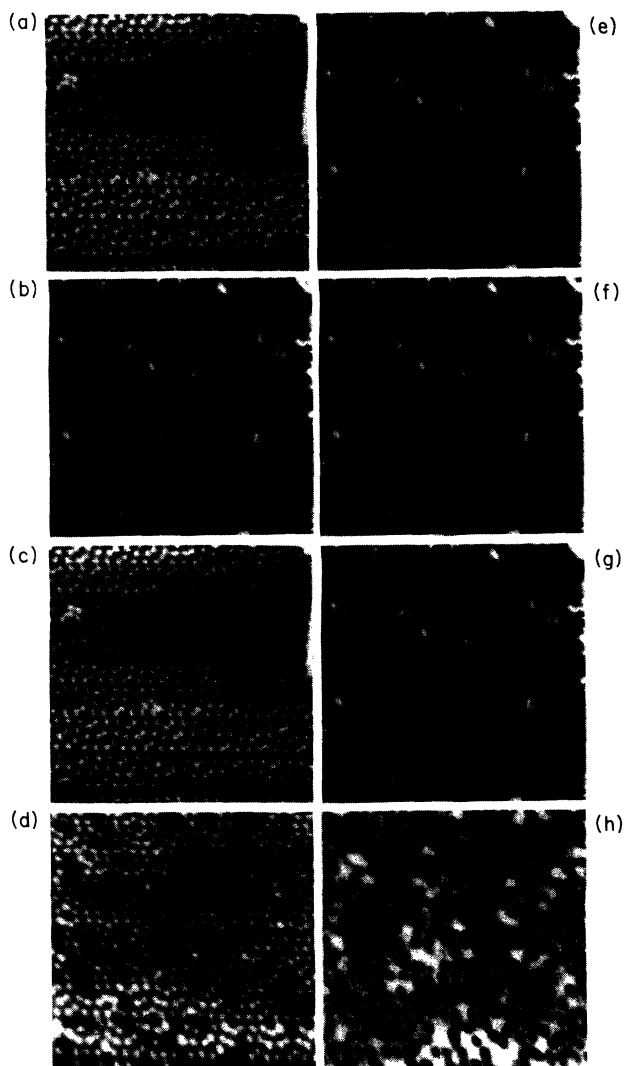


FIG. 1. (a)–(d): Top-view gray-scale topographic images of a particular sample area for 0, 0.1, 0.3, and 0.9 L total oxygen dose, measured with $V_t = -2$ V. (e)–(h) STS images evaluated at $V_t = -2$ V (see text) of the same area measured simultaneously with (a)–(d), respectively. Small \times 's mark four specific locations as position references. Small arrows mark specific sites where $S1$ adatoms were observed after a 0.1-L dose. Faulted half of 7×7 unit cell outlined in lower right corner of (a). Images cover roughly 20×20 nm², but are not corrected for scanner drift or nonorthogonal scanner coupling.

L, where $1 \text{ L} \equiv 10^{-6}$ Torr. The Si atoms seen on the clean surface are called *adatoms*.¹⁸ We note here that the tip lost spatial resolution between the 0.3 and 0.9 L images. However, in this case atomic resolution was regained by allowing the tip to lightly touch the surface. Figures 1(e)–1(h) show a corresponding sequence of STS images taken simultaneously with the topographic images, each a spatial plot of the quantity $[d \ln I_t / d \ln V_t]$ evaluated at $V_t \cong -2$ V. This particular tip was *not* uniform, and hence we will use these spectral images only to indicate changes in the sample DOS at specific atomic sites. The value -2 V was chosen simply because the changes discussed below were most obvious at this voltage.

From Fig. 1(f), we see that after a 0.1-L dose of O₂, small white patches appear on the image, indicating that the DOS of the sample has *changed* at specific locations, each centered on a position occupied by an adatom. This indicates that these specific adatoms have reacted. We shall call such reacted adatoms “stage-1” ($S1$) adatoms. The small arrows in the images point to nine specific locations where $S1$ adatoms were seen after the 0.1 L dose.

When $D_T = 0.3$ L, Fig. 1(g) indicates additional $S1$ adatoms have been created, while Fig. 1(c) shows at several locations what looks similar to “missing adatoms” which we shall call “stage-2” ($S2$) adatoms. Furthermore, by carefully comparing the 0.1 and 0.3 L images, we find at *every* position where an $S1$ adatom was observed in the 0.1-L images, either that an $S1$ adatom is still present (indicated by a white patch in the STS image), or that it has further reacted into an $S2$ adatom (i.e., a “missing” adatom in the topographic images.) Hence, there appears to be a *two-step* reaction process at individual adatom locations. Each step requires an exposure to oxygen; successive images taken without additional O₂ show no creation of $S1$ or conversion to $S2$ adatoms for periods as long as 1 h. The STS image for $D_T = 0.9$ L shown in Fig. 1(h) looks qualitatively different from the other STS images, presumably due to an altered tip spectrum caused by surface contact. Nevertheless, $S1$ adatoms can still be seen as “white patches,” while unreacted adatoms appear as dark round holes. Of the nine $S1$ adatoms noted by arrows when $D_T = 0.1$ L, four have converted to $S2$ when $D_T = 0.3$ L, and two more have converted when $D_T = 0.9$ L.

We also find at low coverages that $S1$ adatoms occur preferentially by roughly a 4:1 ratio on the “faulted” rather than “unfaulted” half of the 7×7 unit cell, and by a 2:1 ratio at “corner” rather than “center” adatom sites.¹⁹ This is apparent from Fig. 1(f). With other tips and samples, we see the same basic sequence of events (i.e., creation of $S1$ -type adatoms at low coverage, conversion of $S1$ to $S2$), and find the same preferred sites. Of 98 $S1$ -type adatoms observed from four different samples at low coverage ($D_T \leq 0.2$ L) we found 56 at faulted-corner sites, 23 at faulted-center sites, 11 at unfaulted-corner sites, and 8 at unfaulted-center sites. At higher coverage, these site preferences appear to be much less pronounced.

Figure 2 shows several possible bonding configurations for atomic oxygen at adatom sites. We propose that an $S1$ reacted adatom corresponds to Fig. 2(c), i.e., a single oxygen atom inserted into a *back-bond* configuration, while an $S2$ adatom has two (or possibly three) oxygen

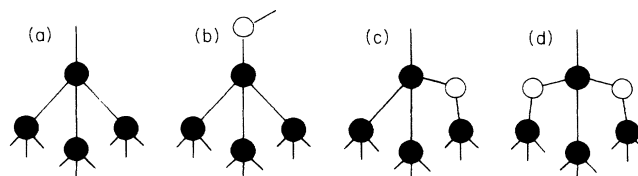


FIG. 2. Several possible adatom bonding configurations. Si (O) atoms shown as filled (empty) circles. (a) Unreacted Si adatom. (b) O atom in on-top configuration. (c) O in back-bond. (d) Two O atoms in backbonds.

atoms in back bonds as in Fig. 2(d). This simple assignment is consistent with our observation of a two-step reaction process, where each step requires exposure to oxygen. It is also consistent with prior electron-energy-loss spectroscopy (EELS),¹ x-ray photoemission (XPS),² and recent transmission electron diffraction (TED) work²⁰ which indicates that atomic oxygen is primarily bonded to two Si atoms (rather than one) even at the earliest oxidation stages. Furthermore, the TED work also indicates that O bonds preferentially at corner adatom back-bond sites, in agreement with our findings. Finally, we note that since the EELS and XPS work indicated that a small ($\approx 20\%$) fraction of the atomic O might be in an "on-top" position at 1-L exposure, it is possible that some of the $S2$ sites have an O on-top as well as in a back bond.

With regard to the observed site preferences, we note that Hamers *et al.*⁸ have observed on the clean 7×7 surface a filled adatom dangling bond (DB) state at ~ 0.3 eV below E_F , which appears more intense in STS images (i.e., has higher occupation) on the faulted (versus unfaulted) half of the unit cell, and at corner (versus center) adatom sites. This ordering of adatom DB intensity on the clean surface is the same as we observe for the adatom reactivity, suggesting that the site preferences are directly related to differences in the adatom electronic states. We do not believe that the site preferences result from different strain energy at the various adatom sites, as has been suggested for the case of NH_3 adsorption⁹ on Si(111). The atomic positions (and hence the atomic strains) in the reconstructed layers of the 7×7 unit cell are known to have near mirror symmetry between the faulted and unfaulted sides.^{21,22} Hence, a strain-related explanation would predict similar reactivities for the faulted and unfaulted sides, in contradiction to our observations.

Semiquantitative spectra at reacted sites can also be obtained from particular scans if the tip can be shown to be uniform. Such spectra would be quite useful in future work, both to compare with electronic structure calculations of particular bonding configurations, and to identify equivalent reacted sites in future experiments. In our scans of the 7×7 surface with submonolayer oxygen coverage, we have determined whether particular tips were uniform by comparing $(d\ln I_t/d\ln V_t)$ measured at unreacted sites with previous STS (Refs. 8 and 9) and photoemission²³ results. If, for a particular tip, the spectra we measure are consistent with previous work, the tip can be considered nominally uniform. We can then use $(d\ln I_t/d\ln V_t)$ to approximate the sample DOS at reacted sites in the same scan.

Figure 3 shows STM and STS images taken with a particular, uniform tip. With a uniform tip, $S1$ adatoms are clearly apparent in both the topographic images shown in Fig. 3(a) (appearing as "raised" or "bright" adatoms) as well as the -2 V STS image shown in Fig. 3(b). We note here that $S1$ adatoms in Fig. 3(b) show quite different relative contrast from that seen in Figs. 1(f)–1(h). As we discuss elsewhere,¹⁷ this, to a large extent, can be understood in terms of particular differences in the DOS of the respective tips. Curves A–C in Fig. 4 show I - V data taken simultaneously with Fig. 3(c), for the tip positioned

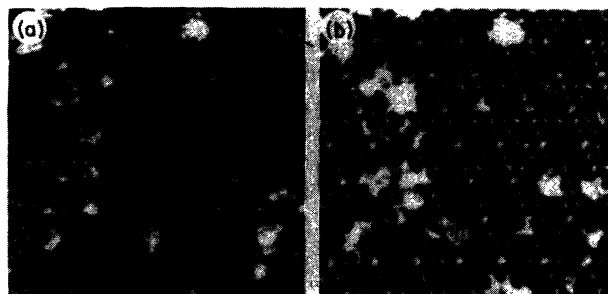


FIG. 3. Topographic images and STS images measured with uniform tip. (a) Topographic images ($V_t = -2$ V) of surface exposed to 0.2-L O_2 . (b) Simultaneous STS image with $V_t = -2$ V. Small arrows mark specific O_2 -induced $S1$ sites. Large "blobs" in images are contamination of unknown origin present on the surface before O_2 exposure.

above unreacted "rest-atom" sites,¹⁹ unreacted adatoms, and (reacted) $S1$ adatoms, respectively. The curves for the unreacted rest atom and adatom correlate well with previous spectral results^{8,9,13,23} indicating that this tip is approximately uniform. Therefore, the solid curve C in Fig. 4 should resemble the actual electronic spectrum at $S1$ sites. Curves D–F in Fig. 4 show data taken from a different sample and uniform tip. A comparison of curves A–C with D–F shows to what extent the measured spectra are reproducible. Compared with unreacted adatoms, we see with both tips the following features at $S1$ sites: (1) a reduction in the DOS close to the Fermi level, (2) peaks in the DOS at $\sim \pm 0.7$ eV, and (3) a shoulder at $\sim +0.3$ eV, and a reduction in the DOS at $\sim +1.5$ eV. These specific features can be used to identify chemically

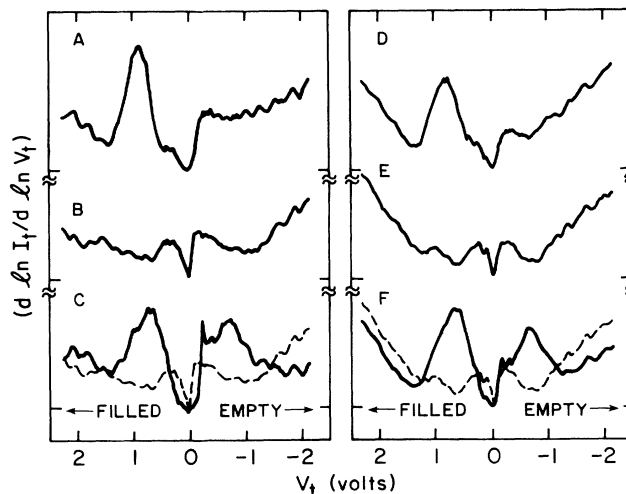


FIG. 4. I - V data acquired with two uniform tips. Curves A–C acquired simultaneously with Fig. 3 above, with tip positioned over unreacted rest-atom sites (curve A), unreacted adatoms (curve B), and $S1$ adatoms (curve C). Curve B replotted as dashed curve in C for direct comparison. Curves D–F: Data from single scan acquired with different tip and sample, with tip over equivalent sites as in curves A–C, respectively. Data from 6–8 equivalent sites averaged for each curve.

equivalent reacted sites in future experiments, and can be compared with calculated spectra. We also note that features (1) and (2), in particular, are consistent with a scenario in which oxygen atoms inserted into back bonds open up an energy gap at the Fermi level. Spectra measured at *S*2 sites (not shown) do not show well-defined peaks close to the Fermi level, in qualitative agreement with this scenario.

Finally, we note that two groups have previously used STM (but not STS) to study oxidation of the 7×7 surface.^{10,11} In several respects, our topographic images are qualitatively consistent with previous work, where "missing adatoms" are observed to appear and grow into spatially correlated patches. As previously reported,¹⁰ we have also occasionally observed the "reappearance" of missing adatoms. However, the previous workers did not report a two-step reaction process or the equivalent of *S*1-type adatoms, and observed a significantly lower probability for the creation of *S*2-type ("missing") adatoms than we see. We plan further experiments to investigate possible causes of these differences in behavior.

In summary, we have observed a two-stage oxidation of adatoms on the Si(111) 7×7 surface, which we suggest correspond to Si adatoms back bonded to one or two oxygen atoms, respectively. At low coverage, the first stage shows a strong preference for the faulted half and the corners of the 7×7 unit cell. At these reacted sites, STS measurements made with uniform tips show energy-level shifts of $\sim \frac{1}{2}$ eV, and a small Fermi-level gap. Stage-2 adatoms appear similar to "missing" adatoms in empty-state topographic images.

Note added in proof. Another group²⁴ has recently made independent STM and STS measurements similar to those discussed here.

We would like to thank R. Hamers for the use of image-processing software and helpful advice, and D. Abraham, J. Boland, J. Clabes, J. Demuth, R. Laibowitz, I.-W. Lyo, K. Markert, and A. Samsavar for useful discussions.

¹A. J. Schell-Sorokin and J. E. Demuth, *Surf. Sci.* **157**, 273 (1985).

²G. Hollinger, J. F. Morar, F. J. Himpsel, G. Hughes, and J. L. Jordan, *Surf. Sci.* **168**, 609 (1986).

³P. Gupta, C. H. Mak, P. A. Coon, and S. M. George, *Phys. Rev. B* **40**, 7739 (1989).

⁴S. Ciraci, S. Ellialtioglu, and S. Erkoç, *Phys. Rev. B* **26**, 5716 (1982).

⁵I. P. Batra, P. S. Bagus, and K. Hermann, *Phys. Rev. Lett.* **52**, 384 (1984).

⁶G. Binnig, H. Rohrer, Ch. Gerber, and E. Weibel, *Phys. Rev. Lett.* **49**, 57 (1982).

⁷R. M. Feenstra, W. A. Thompson, and A. P. Fein, *Phys. Rev. Lett.* **56**, 608 (1986).

⁸R. J. Hamers, R. M. Tromp, and J. E. Demuth, *Phys. Rev. Lett.* **56**, 1972 (1986).

⁹Ph. Avouris and R. Wolkow, *Phys. Rev. B* **39**, 5091 (1989).

¹⁰F. M. Leibsle, A. Samsavar, and T.-C. Chiang, *Phys. Rev. B* **38**, 5780 (1988).

¹¹H. Tokumoto, *J. Vac. Sci. Technol. A* **8**, 255 (1990).

¹²K. Besocke, *Surf. Sci.* **181**, 145 (1987).

¹³R. J. Hamers, *Annu. Rev. Phys. Chem.* **40**, 531 (1989).

¹⁴R. M. Feenstra, J. A. Stroscio, and A. P. Fein, *Surf. Sci.* **181**, 295 (1987).

¹⁵R. M. Tromp, E. J. van Loenen, J. E. Demuth, and N. D. Lang, *Phys. Rev. B* **37**, 9042 (1988).

¹⁶I.-W. Lyo and Ph. Avouris, *Science* **245**, 1369 (1989).

¹⁷J. P. Pelz and R. H. Koch (unpublished).

¹⁸K. Takayanai, Y. Tanishiro, M. Takahashi, H. Motoyoshi, and K. Yagi, *J. Vac. Sci. Technol. A* **3**, 1502 (1985).

¹⁹See Refs. 9 and 18 for a description of the 7×7 reconstruction and related terminology.

²⁰J. M. Gibson, in *Atomic Scale Properties of Interfaces*, MRS Symposia Proceedings Vol. 159 (Materials Research Society, Pittsburgh, 1990), p. 179.

²¹I. K. Robinson, *Phys. Rev. B* **35**, 3910 (1987).

²²G.-X. Quian and D. J. Chadi, *Phys. Rev. B* **35**, 1288 (1987).

²³F. J. Himpsel and Th. Fauster, *J. Vac. Sci. Technol. A* **2**, 815 (1984).

²⁴Ph. Avouris and I.-W. Lyo (unpublished).

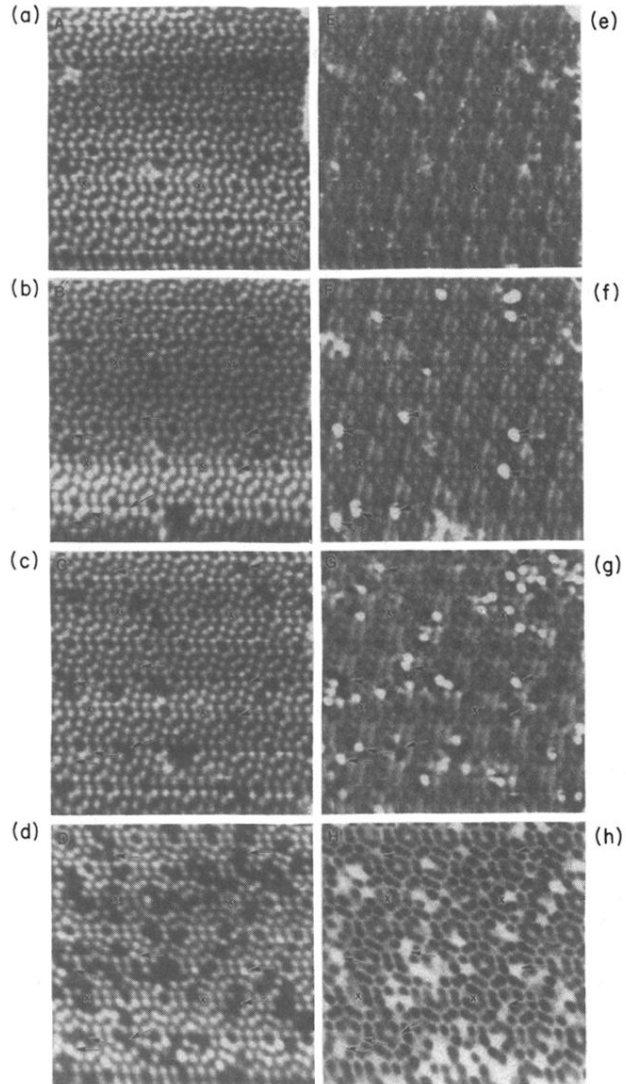


FIG. 1. (a)–(d): Top-view gray-scale topographic images of a particular sample area for 0, 0.1, 0.3, and 0.9 L total oxygen dose, measured with $V_t = -2$ V. (e)–(h) STS images evaluated at $V_t = -2$ V (see text) of the same area measured simultaneously with (a)–(d), respectively. Small \times 's mark four specific locations as position references. Small arrows mark specific sites where $S1$ adatoms were observed after a 0.1-L dose. Faulted half of 7×7 unit cell outlined in lower right corner of (a). Images cover roughly 20×20 nm², but are not corrected for scanner drift or nonorthogonal scanner coupling.

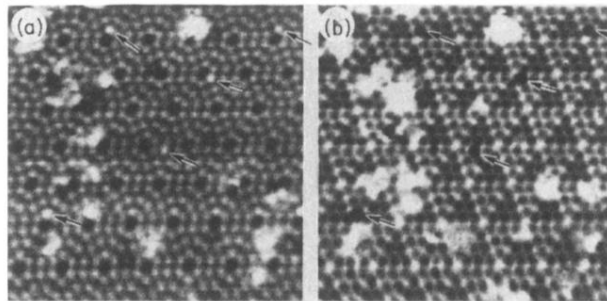


FIG. 3. Topographic images and STS images measured with uniform tip. (a) Topographic images ($V_t = -2$ V) of surface exposed to 0.2-L O_2 . (b) Simultaneous STS image with $V_t = -2$ V. Small arrows mark specific O_2 -induced $S1$ sites. Large “blobs” in images are contamination of unknown origin present on the surface before O_2 exposure.